3,5-Diiodo-L-thyronine prevents high-fat-diet-induced insulin resistance in rat skeletal muscle through metabolic and structural adaptations

Maria Moreno,* Elena Silvestri,* Rita De Matteis,† Pieter de Lange,‡ Assunta Lombardi,§ Daniela Glinni,* Rosalba Senese,‡ Federica Cioffi,‡ Anna Maria Salzano,‖ Andrea Scaloni,‖ Antonia Lanni,‡ and Fernando Goglia*,[1]

*Dipartimento di Scienze per la Biologia, la Geologia e l'Ambiente, Università degli Studi del Sannio, Benevento, Italy; †Dipartimento di Scienze Biomolecolari, Università di Urbino Carlo Bo, Urbino, Italy; ‡Dipartimento di Scienze della Vita, Seconda Università degli Studi di Napoli, Caserta, Italy; §Dipartimento delle Scienze Biologiche, Sez. Fisiologia ed Igiene, Università degli Studi di Napoli Federico II, Naples, Italy; and ‖Laboratorio di Proteomica e Spettrometria di Massa, Instituto per Il Sistema Produzione Animale in Ambiente Mediterraneo, Consiglio Nazionale delle Ricerche, Naples, Italy

ABSTRACT **The worldwide prevalence of obesity-associated pathologies, including type 2 diabetes, requires thorough investigation of mechanisms and interventions. Recent studies have highlighted thyroid hormone analogs and derivatives as potential agents able to counteract such pathologies. In this study, in rats receiving a high-fat diet (HFD), we analyzed the effects of a 4-wk daily administration of a naturally occurring iodothyronine, 3,5-diiodo-L-thyronine (T2), on the gastrocnemius muscle metabolic/structural phenotype and insulin signaling. The HFD-induced increases in muscle levels of fatty acid translocase (3-fold; $P<0.05$) and TGs (2-fold, $P<0.05$) were prevented by T2 (each; $P<0.05$ *vs.* HFD). T2 increased insulin-stimulated Akt phosphorylation levels (~2.5-fold; $P<0.05$ *vs.* HFD). T2 induced these effects while sparing muscle mass and without cardiac hypertrophy. T2 increased the muscle contents of fast/glycolytic fibers (2-fold; $P<0.05$ *vs.* HFD) and sarcolemmal glucose transporter 4 (3-fold; $P<0.05$ *vs.* HFD). Adipocyte differentiation-related protein was predominantly present within the slow/oxidative fibers in HFD-T2. In T2-treated rats (*vs.* HFD), glycolytic enzymes and associated components were up-regulated (proteomic analysis, significance limit: 2-fold; $P<0.05$), as was phosphofructokinase activity (by 1.3-fold; $P<0.05$), supporting the metabolic shift toward a more glycolytic phenotype. These results highlight T2 as a potential therapeutic approach to the treatment of diet-induced metabolic dysfunctions.—Moreno, M., Silvestri, E., De Matteis, R., de Lange, P., Lombardi, A., Glinni, D., Senese, R., Cioffi, F., Salzano, A. M., Scaloni, A., Lanni, A., Goglia, F. 3,5-Diiodo-L-thyronine prevents high-fat diet-induced insulin resistance in rat skeletal muscle through metabolic and structural adaptations. *FASEB J.* 25, 3312–3324 (2011). www.fasebj.org**

Key Words: thyroid hormone · metabolism · proteomics

FAT ACCUMULATION WITHIN tissues has deleterious consequences for organ function and may lead to metabolic disorders such as insulin resistance (IR), type 2 diabetes, heart disease, and hypertension. Several strategies aim to combat these events by limiting the inappropriate deposition of fat within peripheral tissues. In this context, research on skeletal muscle (SKM) is attractive because of that tissue's integral role in regulating whole-body glucose/lipid homeostasis. In fact, ~80% of ingested glucose is taken up by SKM and either oxidized to provide energy or stored as glycogen (1). Moreover, fatty acid oxidation within SKM satisfies a large part of the energy requirements of this tissue in the resting state (2). Under situations of fat overload, such as during high-fat feeding, SKM is faced with increasing amounts of lipids that it is unable to oxidize, and these therefore accumulate, leading to derangements in insulin signaling and to muscle and, indeed, to systemic insulin resistance (3). This condition plays a key role in the metabolic disorders associated with obesity, thus contributing to the development of the metabolic syndrome (4). The mechanisms underlying muscle insulin resistance have not yet been fully elucidated, although they seem to involve derangements in lipid metabolism and lipotoxicity (1–11), alterations in the PI3K/Akt pathway (12–16), and skeletal muscle fiber type (17–20).

Most effort has been directed at reducing the accumulation of detrimental lipids within muscle and liver by decreasing the availability of triglycerides (TGs) and nonesterified fatty acids *via* the circulation. This can be done by using either or both of the classic preventive strategies (reducing caloric intake and/or increasing

[1] Dipartimento di Scienze per la Biologia, la Geologia e l'Ambiente, Università degli Studi del Sannio, via Port'Arsa 11, 82100 Benevento, Italy. E-mail: goglia@unisannio.it

doi: 10.1096/fj.11-181982

0892-6638/11/0025-3312 © FASEB

physical activity). A number of therapeutic options are currently available for the treatment of metabolic disorders, but because of the existence of some unwanted side effects, the development of safer and more effective agents is still a major priority.

Thyroid hormone (TH) is an important modulator of lipid metabolism and metabolic rate, favoring lipolysis and increasing the use of fatty acids as fuels, effects that have the desirable result of reducing fat accumulation (21). A number of investigations have demonstrated stimulatory effects of triiodothyronine (T3) on insulin-stimulated glucose transport and/or phosphorylation in muscle (22, 23), on the insulin-sensitive muscle glucose transporter, namely glucose transporter 4 (GLUT4; 22, 24), and on glycolysis in isolated muscle (23). Other, consistent data have shown decreased insulin-stimulated glucose transport and/or phosphorylation, as well as a lower rate of glycolysis in isolated muscles from hypothyroid animals (25). Because of the induction of adverse side effects (mostly at the cardiac level), the use of TH as an adiposity counteractor has been greatly limited.

We showed that a natural TH derivative, namely 3,5-diiodo-L-thyronine (T2), has the potential to prevent adiposity when administered to rats receiving a high-fat diet (HFD) without the undesirable side effects attributed to THs (26), and they were accompanied at the cellular level by an increase in fatty acid oxidation in the liver, and reductions in the circulating levels of cholesterol and TGs (26). These actions may ultimately reduce the amount of lipids available to skeletal muscle, thus counteracting the fat-induced IR attributable to an HFD. To test the above idea, we designed this study to investigate the capacity of T2 to counteract HFD-linked muscle IR in rats. To that end, we directly assessed the effects of T2 on muscle insulin signaling; the muscle content of lipids and TGs; the muscle fiber type profile; the sarcolemmal levels of Akt, fatty acid translocase (FAT/CD36), and GLUT4; the muscle proteomic profile; and the fiber-specific localization of adipocyte differentiation-related protein (ADRP).

MATERIALS AND METHODS

Animals

Male Wistar rats (aged 8 wk) were purchased from Charles River (Lecco, Italy). They were housed in individual cages in a temperature-controlled room at 28°C (thermoneutral temperature for rats) with a 12-h light-dark cycle. A commercial mash (Charles River) was available *ad libitum*, and the animals also had free access to water.

At the beginning of this study, which was after 7–10 d of acclimatization (d 0), rats were divided into 3 groups (15 animals/group). In each group, body weight was normally distributed, and group means were similar (300±5 g). The first group (N group) was fed a standard diet (Muscedola s.r.l., Milan, Italy); the total metabolizable percentage of energy was made up as follows: 60.4% carbohydrates, 29% proteins, and 10.6% fat, J/J (15.88 kJ gross energy/g). The second group (HFD group) was fed an HFD; the total metabolizable percentage of energy was made up as follows: 21% carbohydrates, 29% proteins, and 50% fat, J/J (19.85 kJ gross energy/g; 26). The third group (HFD-T2 group) received the above HFD together with a daily intraperitoneal injection of T2 (25 μg/100 g body weight). N and HFD rats were sham-injected. Each group was divided into 3 subgroups of 5 rat. Ten rats were subjected to food deprivation for 5 h and were subsequently injected with either insulin (10 U/kg body weight; 5 rats) or saline (5 rats) for the determination of insulin-stimulated Akt phosphorylation. The remaining rats were used for all other measurements.

Animal care and experiments were conducted in accordance with the guidelines issued by the Italian Ministry of Health. At the end of the treatments, rats were anesthetized by an intraperitoneal injection of chloral hydrate (40 mg/100 g body weight) and were then killed by decapitation. Gastrocnemius muscles were excised, weighed, and either immediately processed or stored at −80°C for later processing.

Metabolic measurements

Total lipid and TG content of muscle were determined by means of an Infinity kit (Sigma-Aldrich Corp., St. Louis, MO). Protein levels of Akt and phosphorylated Akt (Ser-473 were determined in the supernatants of ultracentrifuged gastrocnemius lysates. Polyclonal antibodies were used for this purpose (27). Phosphofructokinase (PFK) was assayed by the method described by Opie and Newsholme (28), except that nonspecific oxidation of nicotinamide adenine dinucleotide hydroxide was inhibited by 1 mM potassium cyanide (27). The serum levels of cholesterol and TGs were determined by following standard procedures. Thyroid hormone levels were determined using materials and protocols supplied by Byk-Sangtec Diagnostica (Hessen, Germany).

Muscle samples were fixed by overnight immersion in 4% formaldehyde and 0.1 M sodium phosphate buffer (PB), pH 7.4. After a brief wash in PB, tissues were either dehydrated and paraffin embedded or immersed in sucrose (30% w/v; with 0.1% sodium azide) and were then embedded in Tissue-Tek (Sakura Finetek Europe, Zoeterwoude, The Netherlands) and immediately frozen in liquid N_2-cooled isopentane. For immunohistochemical analysis, adjacent serial sections (4 μm) were cut, collected onto uncoated glass slides, and used to stain ADRP, GLUT4, and myosin heavy chain type I (MHC Ib) and type II (MHC IIb). The following antibodies were used: anti-ADRP (guinea pig polyclonal, RDI-PROGP40, 1:5000; Fitzgerald Industries RDI Division, Concord, MA, USA), anti-GLUT4 (rabbit polyclonal, 1:100; Abcam, Cambridge, UK), anti-fast myosin (clone MY-32, monoclonal, 1:4000; Sigma-Aldrich Corp.), and anti-slow myosin (clone NOQ7.5.4D, monoclonal, 1:6000; GeneTex, Irvine, CA, USA). Bound antibody was finally stained by the ABC peroxidase (Vector Laboratories, Burlingame, CA, USA) method. Peroxidase activity was revealed by incubation with 3,3′-diaminobenzidine tetrahydrochloride as substrate. Nuclei were counterstained with hematoxylin, and the sections were mounted in Eukitt (Kindler, Freiburg, Germany). Control sections for nonspecific staining were subjected to the same incubation protocol but with the primary antibody omitted.

To study the fiber type-specific ADRP content, double-staining was performed. Sections processed for ADRP staining (as described above) were washed in running tap water, incubated in PBS for 5 min, and subsequently incubated with monoclonal anti-fast myosin (clone MY-32, dilution 1:4000; Sigma-Aldrich). The immunoreaction was detected by means of a different visualization system from that described above, using an ABC-AP reagent (Vectastain ABC-AP Standard Kit; Vector Laboratories) and Vector Blue Alkaline Phosphatase

Substrate Kit III as the alkaline phosphatase substrate solution (Vector Laboratories). Gray-stained fibers were classified as type II fibers, whereas unstained fibers were classified as type I fibers. The fiber type-specific ADRP-immunoreactive lipid droplet content was valuated by counting the number of ADRP-stained fibers for either slow and fast fibers. Approximately 3000 fibers were individually counted in each experimental group (n=4).

Immunohistochemical fiber type determination

Muscle fiber types were classified as fiber types I and II on the basis of myosin monoclonal antibody immunostaining. Several adjacent serial cross-sections (from each rat) were examined for fast and slow MHC expression. Entire cross-sectional areas were photographed and collected at ×20. Then, recomposed tissue sections stained with slow and fast myosin-directed antibodies were compared to confirm the position of each fiber. Muscle fiber composition was determined by counting the number of positive fibers stained exclusively for either slow or fast myosin. Muscle fibers expressing multiple MHC isoforms were taken to indicate a transitional MHC phenotype and were counted as mixed (fast/slow myosin). Approximately 4000 fibers were individually counted in each experimental group. To confirm colocalization of slow and fast MHCs within fibers, a double-labeling protocol was designed using the above antibodies against fast and slow myosin, each with a different visualization system. In brief, slow myosin was visualized as blue/gray type I fibers, using an SG Substrate Kit (Vector Laboratories) for peroxidase and alkaline phosphatase-conjugated antibody, whereas fast myosin was visualized as pink type II fibers, using a Red Alkaline Phosphatase Substrate Kit I (Vector Laboratories). Fibers expressing multiple MHC isoforms appeared as a pale greyish-pink color (29).

Staining of lipid droplets

Muscle cryosections (6 μm) obtained using a Leica CM1850 cryostat (Leica Microsystems, Wetzlar, Germany) at −29°C were collected onto room-temperature glass slides; lipid droplets were stained by means of a neutral lipid dye [oil red O (ORO)]. ORO staining of muscle cross-sections, combined with immunohistochemistry (fast myosin), has been described previously for the simultaneous visualization of intramyocellular lipids (IMCLs) and identification of the muscle fiber type (30).

Western blotting

Western blot analysis was performed as described previously (27). The following antibodies were used: anti-fast myosin (clone MY-32, monoclonal, 1:4000; Sigma-Aldrich), anti-slow myosin (clone NOQ7.5.4D, monoclonal, 1:6000; GeneTex), anti-GLUT4 (raised in rabbit, polyclonal, 1:50; Cell Signaling Technology, Danvers, MA, USA), and anti-FAT/CD36 (mouse monoclonal FA6-152 to CD36 AB 1744; Abcam]. A β-actin antibody was purchased from Sigma-Aldrich.

Protein extraction and sample preparation for 2-dimensional gel electrophoresis (2-DE)

2-DE was performed essentially as reported previously (31). In brief, frozen muscle tissue (40 mg) was homogenized in 0.25–1 ml of 8.3 M urea, 2 M thiourea, 2% 3-[3-cholamidopropyl) diethylammonio]-1 propane sulfonate, 1% dithiothreitol, and 2% immobilized pH gradient buffer (pH 3–10). The extracts were shaken vigorously for 30 min at 4°C, followed by a 30-min centrifugation at 10,000 *g*. Protein concentration was determined using the detergent-compatible method (DC Protein Assay; Bio-Rad Laboratories, Hercules, CA, USA). Protein extracts were prepared for each animal, and each individual animal was assessed separately. Protein samples (650 μg) were applied to immobilized pH 3–10 nonlinear gradient strips (17 cm; Bio-Rad Laboratories). For each sample, triplicate runs were performed as independent experiments. Focusing started at 200 V; the voltage was gradually increased to 3500 V and then kept constant for a further 66,500 Vh (Protean IEF System; Bio-Rad Laboratories). The second-dimensional separation was performed using 12% SDS-polyacrylamide gels. After protein fixation, the gels were stained with colloidal Coomassie blue (Sigma-Aldrich). Electronic images of the gels were acquired by means of a calibrated GS-800 densitometer (Bio-Rad Laboratories) and analyzed using PDQuest software (Bio-Rad Laboratories). For all spot-intensity calculations, normalized values were used to calculate the relative intensity (RI) for each spot: $RI = v_i/v_t$, where v_i is the volume of the individual spot and v_t the sum of the volumes of all matched spots. Spots with values of $P < 0.05$ and ≥1.5-fold variation in pairwise comparisons were considered to display a significant difference between experimental groups.

Protein digestion and mass spectrometry analysis

Spots from 2-DE were excised from gels, S-alkylated, and digested with trypsin as reported previously (32). Digests were desalted on μZipTipC18 (Millipore Corp., Billerica, MA, USA) before mass spectrometry analysis. During matrix-assisted laser desorption ionization/time of flight (MALDI-TOF) peptide mass fingerprinting (PMF) experiments, peptide mixtures were loaded on the instrument target with α-cyano-4-hydroxycinnamic acid as matrix, using the dried droplet technique. Samples were analyzed on a Voyager-DE PRO mass spectrometer (Applied Biosystems, Foster City, CA, USA). Spectra were acquired in reflectron mode; internal mass calibration was performed using peptides from trypsin autoproteolysis. Data were elaborated using DataExplorer software (Applied Biosystems). Digests were eventually analyzed by nano-liquid chromatography-electrospray ionization-linear ion trap-tandem mass spectrometry (nLC-ESI-LIT-MS/MS) using a LTQ XL mass spectrometer (Thermo Fisher Scientific, Waltham, MA, USA) equipped with a Proxeon nanospray source connected to an Easy-nLC system (Thermo Fisher Scientific; ref. 33). Peptide mixtures were separated on an Easy C_{18} column (10×0.075 mm, 3 μm; Thermo Fisher Scientific) using a gradient of acetonitrile containing 0.1% formic acid in aqueous 0.1% formic acid; acetonitrile was ramped from 5 to 35% over 10 min and from 35 to 95% over 2 min and remained at 95% for 12 min, at a flow rate of 300 nl/min. Spectra were acquired in the range of m/z 400–2000. Acquisition was controlled by a data-dependent product ion-scanning procedure over the three most abundant ions, enabling dynamic exclusion function.

Protein identification

MASCOT 2.2.06 software (Matrix Science Ltd., London, UK; ref. 34) was used to identify spots from a *Rattus norvegicus* sequence database (National Center for Biotechnology Information no. 2010/08/07). MALDI-TOF PMF data were searched using a mass tolerance value of 50 ppm, with trypsin as the proteolytic enzyme, a missed-cleavage maximum value of 2, and Cys carbamidomethylation and Met oxidation as fixed and variable modifications, respectively. nLC-ESI-LIT-

TABLE 1. *Serum component and body weight parameters in rat groups*

Parameter	N	HFD	HFD-T2
Cholesterol (mg/dl)	65.5 ± 0.6	78.5 ± 0.6*	62.5 ± 0.5#
TGs (mg/dl)	105 ± 8.0	250 ± 22.5*	140 ± 18#
Free thyroxine (ng/dl)	0.89 ± 0.09	0.85 ± 0.08	0.80 ± 0.07
Free T3 (pg/ml)	2.00 ± 0.3	2.20 ± 0.2	2.18 ± 0.2
BW (g)	400 ± 12	452 ± 10*	402 ± 11
HW/BW (mg/g)	0.26 ± 0.019	0.24 ± 0.004	0.24 ± 0.008
GW/BW (mg/g)	0.55 ± 0.015	0.56 ± 0.014	0.54 ± 0.022

Data are means ± SE for 5 rats/group. BW, body weight; HW, heart weight; GW, gastrocnemius weight. *$P < 0.05$ *vs.* N rats; #$P < 0.05$ *vs.* HFD rats.

MS/MS data were searched using the same criteria but with a mass tolerance value of 2 Da for the precursor ion and 0.8 Da for MS/MS fragments. MALDI-TOF PMF candidates with a cumulative MASCOT score > 83 or nLC-ESI-LIT-MS/MS candidates with >2 assigned peptides with an individual MASCOT score > 30, both corresponding to $P < 0.05$ for a significant identification, were further evaluated for their experimental mass and pI values obtained from 2-DE. Protein identification was checked with a reverted sequence database to provide a false-positive rate of 1%.

Statistical analysis

Results are expressed as means ± SE. The statistical significance of differences between groups was determined using 1-way ANOVA followed by a Student-Newman-Keuls test. Differences were considered significant at $P < 0.05$.

RESULTS

T2 prevents HFD-induced hyperlipidemia without inducing a thyrotoxic state

Serum levels of cholesterol and TGs were higher in HFD rats than in N rats, whereas in HFD-T2 rats, they were significantly reduced (*vs.* HFD; **Table 1**). In addition, as a control for biological effect, heart weight/body weight and gastrocnemius weight/body weight ratios were determined. T2 treatment, while preventing body weight gain (Table 1), did not change either of these ratios (Table 1), and no change in heart rate was observed on T2 administration (actual beats/min of 300±32, 312±40, and 315±30 in N, HFD, and

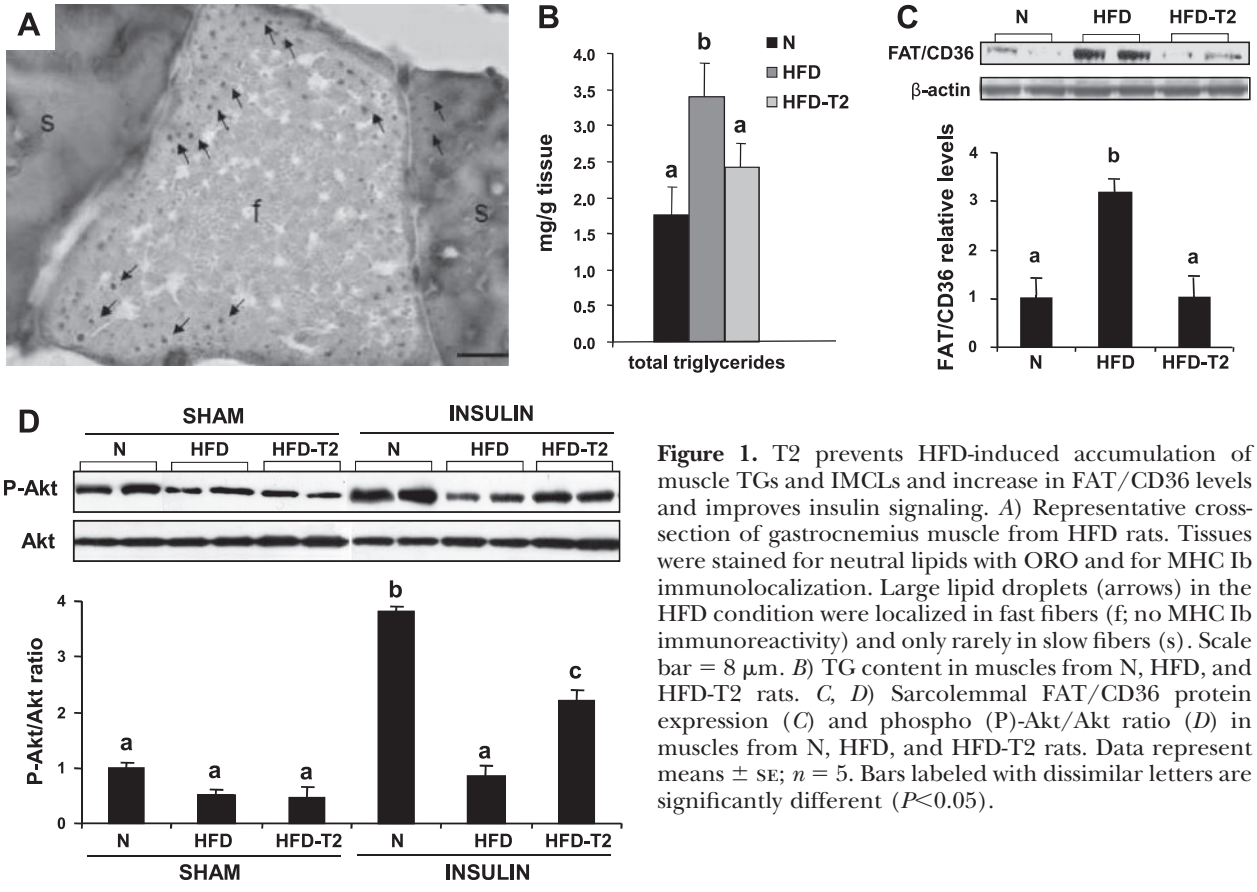

Figure 1. T2 prevents HFD-induced accumulation of muscle TGs and IMCLs and increase in FAT/CD36 levels and improves insulin signaling. *A*) Representative cross-section of gastrocnemius muscle from HFD rats. Tissues were stained for neutral lipids with ORO and for MHC Ib immunolocalization. Large lipid droplets (arrows) in the HFD condition were localized in fast fibers (f; no MHC Ib immunoreactivity) and only rarely in slow fibers (s). Scale bar = 8 μm. *B*) TG content in muscles from N, HFD, and HFD-T2 rats. *C, D*) Sarcolemmal FAT/CD36 protein expression (*C*) and phospho (P)-Akt/Akt ratio (*D*) in muscles from N, HFD, and HFD-T2 rats. Data represent means ± SE; $n = 5$. Bars labeled with dissimilar letters are significantly different ($P<0.05$).

HFD-T2 groups, respectively). No significant difference was found in serum free thyroxine and free T3 levels among the 3 groups (Table 1), in accordance with our previous results (26), showing that in the presence of an unaltered hypothalamus-pituitary-thyroid axis, T2 prevented body weight gain in HFD rats without influencing energy intake, with the changes in body weight being primarily the result of decreases in fat mass, confirming that T2 does not induce thyrotoxic effects.

T2 prevents HFD-induced increases in gastrocnemius muscle TG, IMCL, and FAT/CD36 levels and significantly improves insulin signaling

Skeletal muscles adapt to a given stimulus with structural, biochemical, and functional modifications in line with the fuel used and the energy demand (35). This is particularly true for a mixed-fiber-type muscle, such as gastrocnemius, which contains regions of slow- and fast-twitch fibers. As expected, HFD feeding raised the

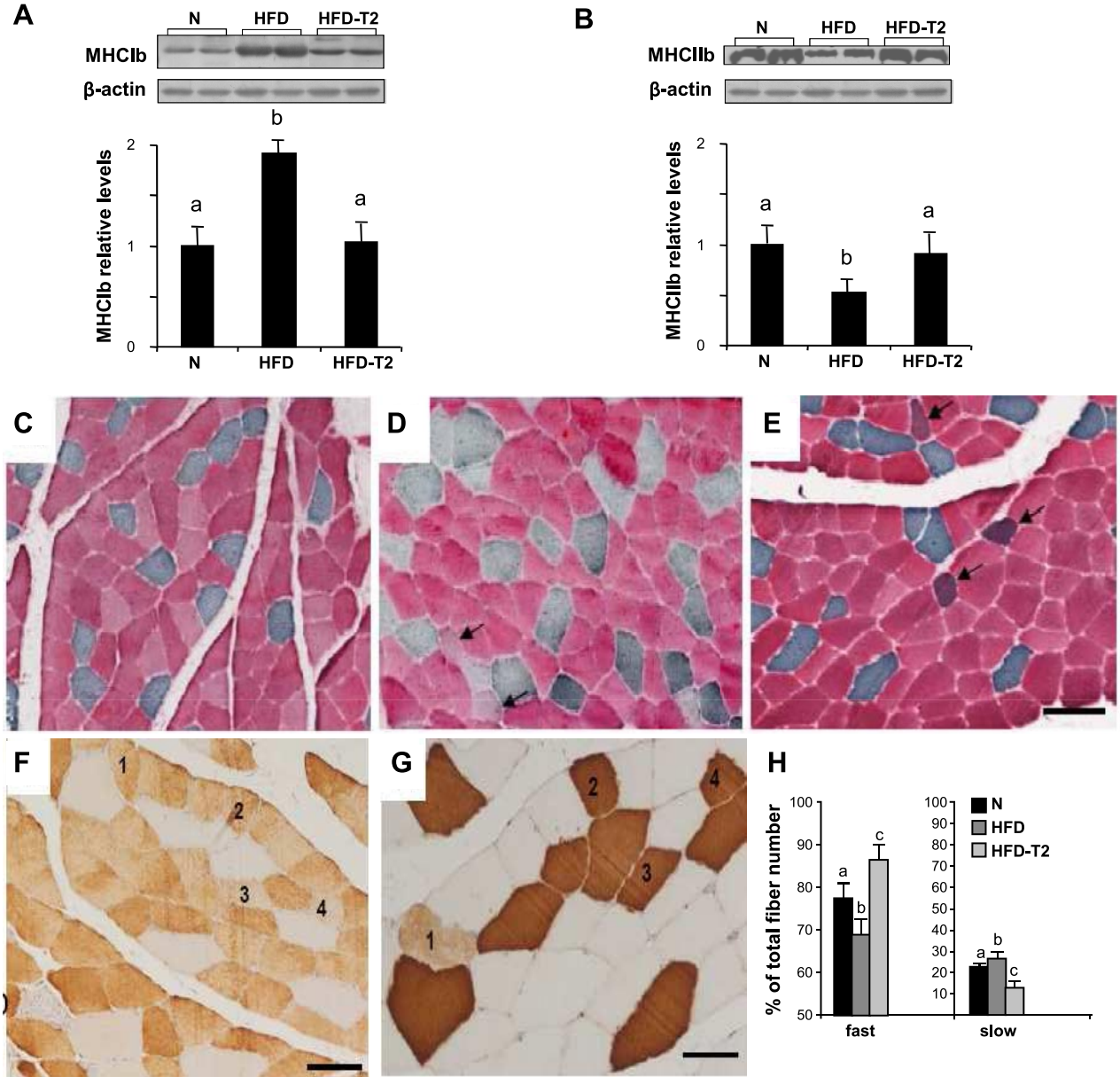

Figure 2. T2 induces a structural shift toward fast/glycolytic myofibers in gastrocnemius muscle. *A–E*) Western blot analyses of MHC Ib (*A*) and MHC IIb (*B*) protein levels, together with representative images of gastrocnemius muscle sections, double-stained by immunohistochemistry for type I (blue-gray) and type IIb (pink) MHC isoforms, from N (*C*), HFD (*D*), and HFD-T2 (*E*) rats. Fibers coexpressing type I and type IIb MHC isoforms (arrows) were identified by their greyish-pink staining. *F, G*) Immunohistochemistry on serial sections of gastrocnemius muscles from HFD-T2 rats for type IIb (*F*) and type I (*G*) MHC showed that most fibers were "pure," containing only the IIb (*F*) or only the I (*G*) MHC isoform. Fibers 1–4 were "hybrids," containing both I and IIb MHC isoforms. Some showed a weaker staining for one type, *e.g.*, type I (fiber 1) or type IIb (fibers3 and 4) MHC isoforms. *H*) Quantitative analysis of gastrocnemius fiber composition (shown as percentage of total fiber number). Data represent means ± SE; $n = 5$. Bars labeled with dissimilar letters are significantly different ($P<0.05$). Scale bars = 100 μm (*C, D, E*); = 83 μm (*F, G*).

gastrocnemius content of IMCLs and TGs (**Fig. 1*A*, *B***). Large lipid droplets were noted within muscle fibers in the HFD condition (Fig. 1*A*). Combined ORO staining and MHC Ib immunolocalization showed that those large lipid droplets (Fig. 1*A*, arrows) were localized to fast fibers. This augmented IMCL accumulation was associated with an elevated basal sarcolemmal-associated FAT/CD36 level (~3-fold *vs.* N; Fig. 1*C*). T2 treatment normalized muscle TG levels (Fig. 1*B*) and prevented the increase in the sarcolemmal FAT/CD36 protein level (Fig. 1*C*), when compared with HFD rats, in the absence of any increase in fatty acid oxidation (data not shown). Therefore, it appears that under HFD conditions, gastrocnemius responds by maintaining a higher concentration of FAT/CD36 on the cell membrane; as a consequence, uptake of fatty acids is increased, and they are stored as IMCLs. By reducing the fatty acid uptake, T2 evidently leads to decreases in IMCL and TG levels in muscle. This result suggests a protective role for T2 in preventing IMCL accumulation and consequently ameliorating the condition of IR induced by the HFD. Indeed, under *in vivo* insulin-stimulated conditions, T2 treatment enhanced the concentration of the phosphorylated form of Akt (~2.5-fold; $P<0.05$ *vs.* HFD), demonstrating that it preserves insulin signaling against the deleterious effect of HFD feeding (Fig. 1*D*).

T2 induces in gastrocnemius muscle a structural and biochemical shift toward glycolytic myofibers

Because the skeletal muscle fiber-type profile might play a role in the IR observed in HFD rats, we measured the relative protein expression levels of the MHC isoforms Ib and IIb in gastrocnemius. Western blot analysis revealed that the MHC Ib level was

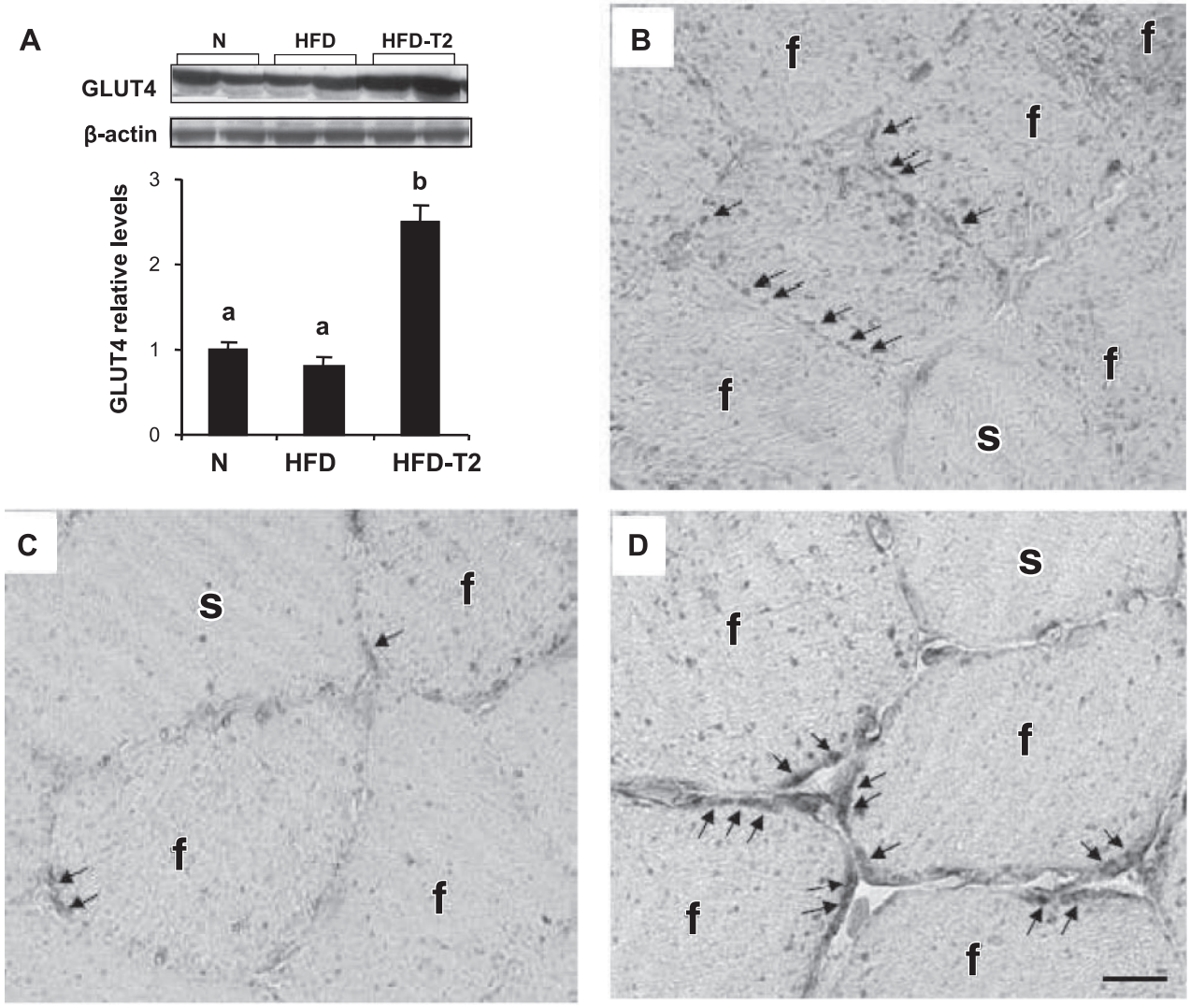

Figure 3. T2 induces an increase in sarcolemmal GLUT4 levels in gastrocnemius muscle. *A*) Western blot analysis of sarcolemmal GLUT4 protein levels. *C–D*) Cell type-specific GLUT4 localization in muscles from N (*B*), HFD (*C*), and HFD-T2 (*D*) rats. GLUT4 immunoreactivity was localized as a scattered granular surface-associated reaction (arrows). s, type I fibers; f, type II fibers. Data represent means ± SE; $n = 5$. Bars labeled with dissimilar letters are significantly different ($P<0.05$). Scale bars = 10 μm.

significantly increased in gastrocnemius from HFD rats, whereas T2 treatment significantly reduced it to the level observed in N rats (**Fig. 2*A***). The MHC IIb level, on the other hand, was significantly reduced in gastrocnemius muscles from HFD rats, but it, too, was restored by T2 treatment (Fig. 2*B*). Quantitative analysis of fiber types revealed that slow/oxidative fibers were replaced to a significant extent by fast/glycolytic fibers after T2 treatment (Fig. 2*C–H*). Of note, although some 4% of fibers were joint fast/slow immunoreactive in both HFD and HFD-T2 rats, the fast component prevailed after T2 treatment (Fig. 2*E, F*), indicating an ongoing structural shift toward the glycolytic phenotype. This shift was supported by the observation that many of the slow/fast immunoreactive fibers were only weakly stained for slow myosin in muscles from HFD-T2 rats (Fig. 2*G*). The sarcolemmal membrane-associated GLUT4 protein content was up-regulated by T2 treatment, in accordance with the observed structural shift (**Fig. 3*A***). The plasma membrane-associated labeling in fast/glycolytic fibers was more intense in the HFD-T2 gastrocnemius

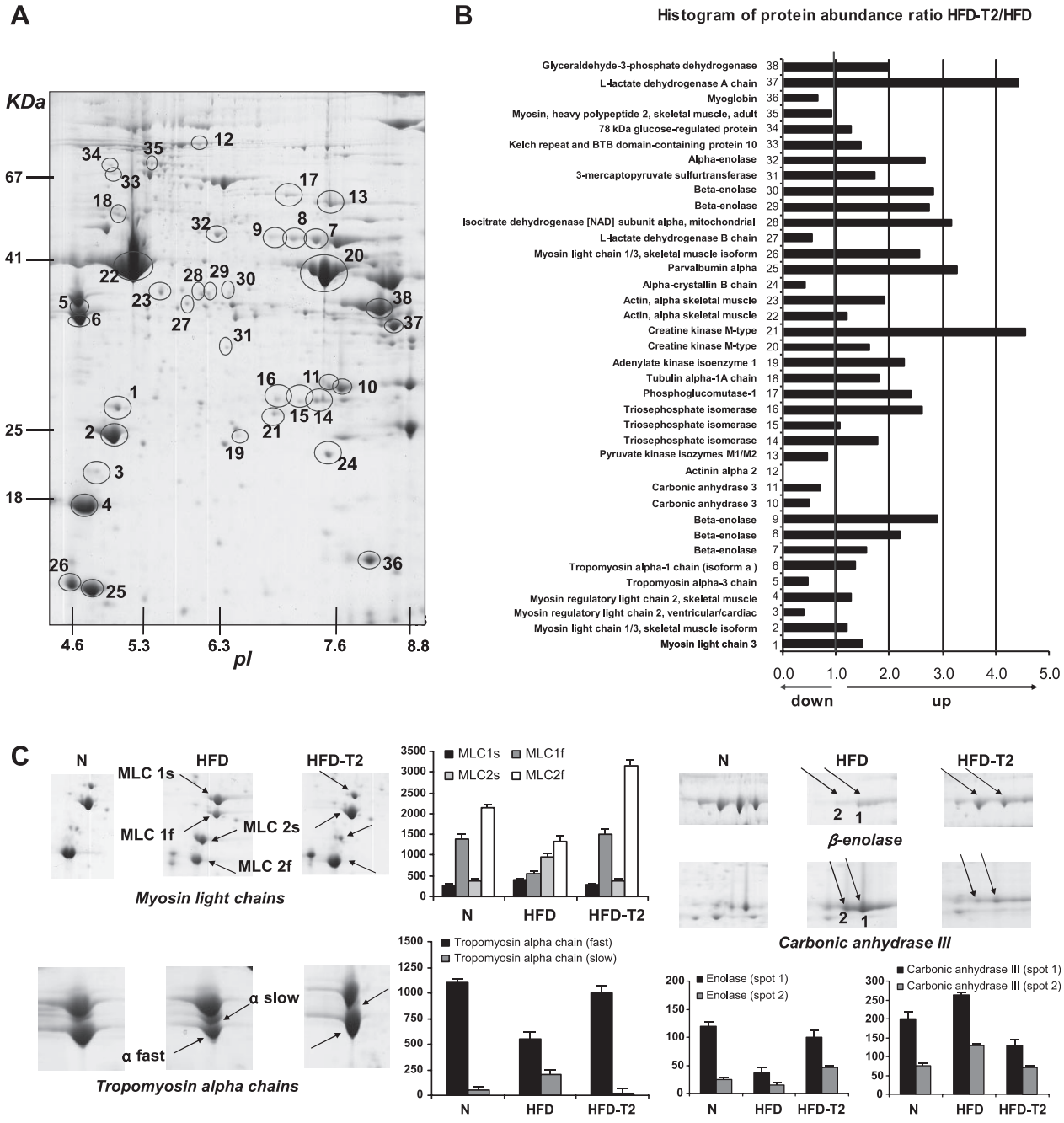

Figure 4. T2 induces a structural and biochemical shift toward the glycolytic phenotype in gastrocnemius muscle. *A*) Gastrocnemius muscle protein profiling by 2-DE. The 38 circled and numbered spots mainly correspond to deregulated protein components after T2 treatment. *B*) Histogram of protein abundance ratio HFD-T2/HFD. *C*) Representative subsections of 2-DE images are shown as examples of differential expression among experimental groups. Data (relative intensity) represent means ± SE; $n = 5$. $P < 0.05$ in pairwise comparisons: HFD *vs.* N; HFD-T2 *vs.* HFD.

(Fig. 3*D*) than in the N (Fig. 3*B*) or HFD (Fig. 3*C*) rats.

To delve more deeply into the effects of long-term T2 treatment on the muscle phenotype, proteomic analysis was performed (**Fig. 4**). The number of proteins identified as significantly differing between HFD-T2 and HFD muscle samples was 38 (Fig. 4*A*, *B* and **Table 2**). Furthermore, several proteins were identified at multiple spot positions, putatively reflecting the occurrence of post-translational modifications. In these cases, however, on average, the changes in the spots were quite similar (Fig. 4*B* and Table 2).

Proteomic analysis revealed that T2 treatment significantly altered the protein expression profile of muscle in the HFD condition. In particular, the protein expression levels of the fast isotypes of myosin light chains (MLC1f, spot2; MLC2f, spot 4) and of the tropomyosin α chain fast (spot 6) increased significantly after T2 treatment, whereas the content of the slow isotypes MLC1s (spot 1) and MLC2s (spot 3) and the tropomyosin α chain slow (spot 5) decreased, in agreement with a shift toward the fast phenotype (Fig. 4*B, C*). Coherently, other proteins, identified as glycolytic enzymes, were all up-regulated in muscles from HFD-T2 rats (*vs.* HFD; Fig. 4*B, C*). These proteins included α- and β-enolase (spots 32 and 30, respectively), which participate in the glycolytic conversion of glucose to pyruvate; phosphoglucomutase-1 (spot 17), an enzyme regulating an important step in both glycolysis and gluconeogenesis; triosephosphate isomerase (spots 14–16), which promotes the formation of glyceraldehyde 3-phosphate molecules to be metabolized further down the glycolytic pathway; glyceraldehyde-3-phosphate dehydrogenase (spot 38), an enzyme yielding NADH from glyceraldehyde 3-phosphate; lactate dehydrogenase (A chain, M type; spot 37), which provides for the interconversion of glycolysis end-products (*i.e.*, pyruvate and lactate) and may regulate the turnover of lactate within the muscle cell; creatine kinase (spots 20 and 21), which, by phosphorylating creatine, plays a crucial energy transduction role; isocitrate dehydrogenase (spot 28); and adenylate kinase isoenzyme 1 (spot 19), which catalyzes the reversible transfer of the terminal phosphate group between ATP and AMP and is involved in energy metabolism and nucleotide synthesis (Fig. 4*A*, *B*).

On the other hand, enzymes involved in oxidative metabolism, such as carbonic anhydrase III (spots 10 and 11) and myoglobin (spot 36), were down-regulated in muscles from HFD-T2 rats compared with those from HFD rats (Fig. 4). The increased levels of glycolytic enzymes in the muscle of HFD-T2 rats were reflected in an increased activity of phosphofructokinase, a key regulatory enzyme for glycolysis (51 ± 3 and 66 ± 4 nmol NADH/min/mg protein for HFD and HFD-T2, respectively). Taken together, these results strongly support biochemical and structural shifts toward the fast glycolytic phenotype in the HFD-T2 gastrocnemius muscle in rats. These shifts parallel the reductions in fatty acid, TG, and cholesterol levels in the serum and the reduced steatosis in the liver reported previously in HFD-T2 rats (26).

T2 increases the localization of ADRP within slow/oxidative fibers

We next investigated another aspect related to intramuscular TG storage, namely ADRP fiber-specific localization. Double-staining MHC IIb and ADRP allowed us to localize fiber type-specific ADRP labeling surrounding IMCLs. The data reported here, in agreement with previous studies (36, 37), showed that the observed ADRP immunoreactivity overlapped well with the lipid staining, demonstrating that this protein is associated with lipid droplets in rat gastrocnemius muscle (**Fig. 5**). In muscle from N rats, ADRP immunoreactivity was poorly evident (Fig. 5*A*) and mainly present around very small lipid droplets located predominantly within slow/oxidative fibers (65.98±5.93% of slow fibers) but also in some fast/glycolytic fibers (24.43±2.38% of fast fibers). In muscle from HFD rats (Fig. 5*B*), the ADRP staining was mainly located around the large lipid droplets present within the fast/glycolytic fibers (41.36± 4.6% of fast fibers); most of them were very intensely ADRP immunoreactive, whereas the few lipid vacuoles located within the slow/oxidative fibers (35.74±5.73% of slow fibers), displayed only very weak ADRP labeling. After T2 treatment, ADRP labeling coated all the IMCLs (Fig. 5*C*); on the whole, slow/oxidative fibers exhibited increased accumulation of ADRP (86.11±4.53 of slow fibers), whereas the fast/glycolytic fibers had a reduced ADRP content (32.83±3.98 of fast fibers).

DISCUSSION

Increased body fat, especially the intramyocellular fat content, has been related to the development of IR (10), a maladaptive response that is currently attributed to the generation of intracellular events that antagonize insulin signaling (38). High-fat feeding has been demonstrated to trigger IR in animal models (39, 40), and the worldwide spread of fat-enriched diets may be the largest contributor to the growing incidence of the metabolic syndrome. Recent interest has focused on therapeutic agents that might be able to improve insulin sensitivity and/or ameliorate the features of metabolic disease by limiting the inappropriate deposition of fat in certain peripheral tissues not suited for lipid storage, such as skeletal muscle. We showed that 4 wk of T2 treatment of HFD rats resulted in a marked prevention of the elevation of plasma free fatty acid levels by increasing hepatic fatty acid oxidation (26). Notably, in contrast to what happens when THs are used as antiobesity agents, T2 treatment did not decrease the skeletal muscle mass and did not affect either heart mass or heart rate, indicating a lack of undesirable side effects associ-

TABLE 2. *Proteins in gastrocnemius muscle with changed expression levels after T2 treatment of HFD rats*

						MALDI-TOF			nLC-ESI-MS/MS		
Spot	SwissProt name	Abbreviation	Accession	Theoretical M_r	Theoretical pI	Peptides matched/ searched (*n*)	Sequence coverage (%)	MASCOT score	Peptides (*n*)	Sequence coverage (%)	MASCOT score
1	Myosin light chain 3	*Myl3*	P16409	22,025	5.03	13/19	70	171	12	81	726
2	Myosin light chain 1/3, skeletal muscle isoform	*Myl1*	P02600	20,548	4.99	18/32	83	199	12	80	863
3	Myosin regulatory light chain 2, ventricular/cardiac muscle isoform	*Myl2*	P08733	18,749	4.86	16/22	71	159	6	35	362
4	Myosin regulatory light chain 2, skeletal muscle isoform	*Mylpf*	P04466	18,838	4.82	24/35	88	265	19	88	1183
5	Tropomyosin α-3 chain	*Tpm3*	Q63610-3	28,875	4.75	20/27	59	224	11	40	678
6	Tropomyosin α-1 chain (isoform a)	*Tpm1*	P04692	32,680	4.69	30/50	68	292	20	61	1105
7	β-Enolase	*Eno3*	P15429	46,882	7.23	14/21	46	176	12	35	732
8	β-Enolase	*Eno3*	P15429	46,882	7.23	12/15	46	155	13	43	790
9	β-Enolase	*Eno3*	P15429	46,882	7.23	7/12	28	87	12	38	667
10	Carbonic anhydrase 3	*Ca3*	P14141	29,300	6.97	15/24	74	215	10	40	594
11	Carbonic anhydrase 3	*Ca3*	P14141	29,300	6.97	20/33	74	263	10	55	580
12	Actinin α 2	*Actn2*	D3ZCV0	103,833	5.31	25/32	30	226	14	22	1022
13	Pyruvate kinase isozymes M1/M2	*Pkm2*	P11980	57,686	6.69	21/35	51	187	26	57	1689
14	Triosephosphate isomerase	*Tpi1*	P48500	26,717	7.06	17/24	73	260	14	67	807
15	Triosephosphate isomerase	*Tpi1*	P48500	26,717	7.06				12	68	784
16	Triosephosphate isomerase	*Tpi1*	P48500	26,717	7.06				10	59	584
17	Phosphoglucomutase-1	*Pgm1*	P38652	61,271	6.32	22/26	49	275	29	59	1927
18	Tubulin α-1A chain	*Tuba1a*	P68370	50,135	4.94	13/37	32	81	15	50	956
19	Adenylate kinase isoenzyme 1	*Ak1*	P39069	21,583	7.66	11/14	61	165	12	72	725
20	Creatine kinase M-type	*Ckm*	P00564	43,045	6.58	33/55	71	316	21	51	1455
21	Creatine kinase M-type	*Ckm*	P00564	43,045	6.58				4	15	291
22	Actin, α skeletal muscle	*Acta1*	P68136	41,816	5.23	20/39	62	187	19	62	1311
23	Actin, α skeletal muscle	*Acta1*	P68136	41,816	5.23	5/7	21	69	10	31	661
24	Alpha-crystallin B chain	*Cryab*	P23928	20,089	6.76	11/20	51	153	13	57	761
25	Parvalbumin α	*Pvalb*	P02625	11,794	5				4	50	233
26	Myosin light chain 1/3, skeletal muscle isoform	*Myl1*	P02600	20,548	4.99	18/32	83	199	13	83	917
27	L-Lactate dehydrogenase B chain	*Ldhb*	P42123	36,481	5.7				15	44	1025
28	Isocitrate dehydrogenase [NAD] subunit α, mitochondrial	*Idh3a*	Q99NA5	36,682	5.72	10/12	28	126	6	21	320
29	β-Enolase	*Eno3*	P15429	46,882	7.23				14	32	874
30	β-Enolase	*Eno3*	P15429	46,882	7.23				9	28	559
31	3-Mercaptopyruvate sulfurtransferase	*Mpst*	P97532	32,809	5.88	6/9	31	96	7	28	423

(*continued on next page*)

TABLE 2. (*continued*)

Spot	SwissProt name	Abbreviation	Accession	Theoretical M_r	Theoretical pI	MALDI-TOF			nLC-ESI-MS/MS		
						Peptides matched/searched (*n*)	Sequence coverage (%)	MASCOT score	Peptides (*n*)	Sequence coverage (%)	MASCOT score
32	α-enolase	*Eno1*	P04764	46,996	6.16	11/16	27	98	20	55	1508
33	Kelch repeat and BTB domain-containing protein 10	*Kbtbd10*	Q9ER30	68,213	5.05	8/12	12		11	29	796
34	78-kDa glucose-regulated protein	*Hspa5*	P06761	70,474	5.01	10/11	20	127	17	33	1156
35	Myosin, heavy polypeptide 2, skeletal muscle, adult	*Myh2*	Q5SX41	219,737	5.63				32	13	2035
36	Myoglobin	*Mb*	Q9QZ76	17,025	7.99				16	83	844
37	L-Lactate dehydrogenase A chain	*Ldha*	P04642	36,319	8.47				11	35	579
38	Glyceraldehyde-3-phosphate dehydrogenase	*Gapdh*	P04797	35,696	8.18				34	67	1234

Spot numbers correspond to Fig. 4*A*, *B*.

ated with the metabolic actions of this iodothyronine. The T2-induced increase in hepatic fatty acid oxidation, and its lowering effects on the levels of plasma lipids, could decrease the supply of fatty acids to muscle cells, relieving lipid overload and leading to increased glucose uptake, thus improving insulin sensitivity (40). The present results show that T2 treatment effectively prevented the HFD-dependent increase in the expression of an important determinant of muscle lipid accumulation and insulin responsiveness, namely FAT/CD36 (5), without significant enhancement of fatty acid oxidation. T2 administration to HFD rats resulted in significant reductions in both IMCL and muscle TG levels, with a concomitant significant stimulation of insulin-induced Akt activation, which is implicated in glucose transport and glycogen synthesis in skeletal muscle cells (15, 41) as well as being implicated in muscle hypertrophy *in vivo* (17), and has been shown to be deregulated in conditions of IR (19, 42). Notably, in the gastrocnemius muscle T2 also caused a slow-to-fast fiber shift, with a concomitant increase in the total Akt protein level (*vs.* HFD rats). This phenomenon is consistent with results published by Izumiya *et al.* (20), who created obese Akt1 transgenic mice that displayed hypertrophy of fast/glycolytic muscle fibers. The growth of fast/glycolytic muscle in these obese mice normalized their responses to exogenous glucose and insulin and reversed their hepatic steatosis (20). These data indicated that increasing the fast muscle size (*e.g.*, *via* strength training) could be an important intervention for the at-risk populations. Indeed, fast muscle fibers are more responsive to resistance training which, in humans, has been linked to reduced adiposity and improved insulin sensitivity and is a recommended mode of exercise for patients with type 2 diabetes (43, 44). It is consistent with all this that the gastrocnemius muscles of HFD-T2 rats were more insulin-sensitive that their HFD equivalents.

Our proteomic analysis confirmed the T2-induced structural shift within the gastrocnemius muscle toward a more glycolytic phenotype in a situation in which the serum levels of TGs, free fatty acids, and cholesterol are lowered by increased hepatic fatty acid oxidation. Indeed, high levels of proteins/enzymes involved in the glycolytic pathway, Krebs' cycle, muscle structure, and glucose transport were detected in gastrocnemius muscles from HFD-T2 rats *vs.* those from HFD rats. The increased levels of glycolytic enzymes, as well as of lactate dehydrogenase (A chain, M type), within the muscles from HFD-T2 rats were reflected by increased phosphofructokinase activity. Such a metabolic shift would lead to a smaller demand for oxygen, and so the observed decrease in the O_2 carrier myoglobin in HFD-T2 muscle agrees well with the notion of decreased oxidative metabolism. Moreover, the higher levels of cytosolic creatine kinase observed in muscle from HFD-T2 rats would support the formation of

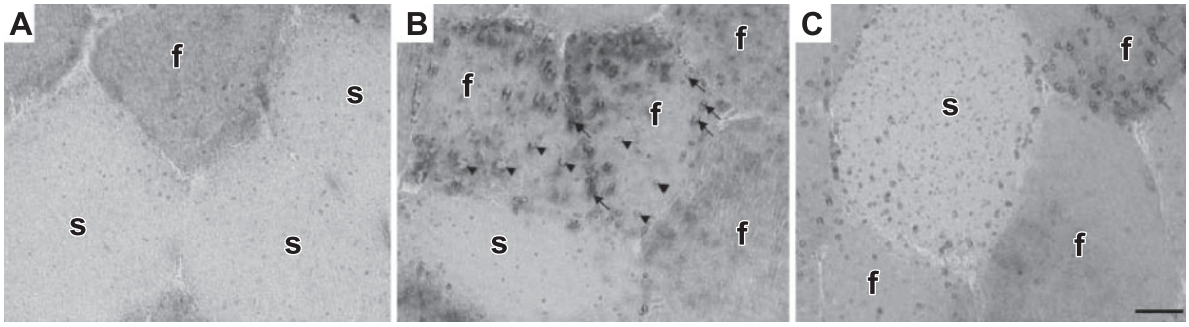

Figure 5. T2 exerts a fiber type-specific effect on the localization of ADRP protein. Double-staining for ADRP (dark gray) and MHC IIb (light gray). *A*) Very small, weakly ADRP-immunoreactive lipid droplets were observed within slow (s) and (rarely) in some fast (f) fibers in the N condition. *B*) In HFD rats, ADRP immunolabeling coated many large lipid droplets intensely (arrows) or weakly (arrowheads) in fast fibers, whereas slow fibers contained small, very weakly ADRP-stained lipid vacuoles. *C*) In HFD-T2 rats, both the number and the diameter of lipid droplets within fast fibers were reduced; some large lipid droplets were also observed (red arrows). Scale bars = 12 μm.

ATP from ADP *via* the use of phosphocreatine and thus increased dependence of energy metabolism on the creatine kinase shuttle in glycolytic muscle.

Such structural and biochemical shifts seem to mimic the reported ability of T3 to convert skeletal muscle fiber type I to type II (45). Notably, however, the effects of T2, but not those of T3, are associated with a sparing of muscle mass. This finding indicates that T2 does not drive sarcopenia and argues strongly in favor of the potential utilization of T2, rather than T3, as a therapeutic option to counteract overweight and the associated metabolic derangements.

Another factor that appears to be affected by T2 treatment is fiber type-specific IMCL deposition. In particular, the ability of T2 to prevent HFD-induced lipid accumulation within glycolytic fibers, which has been shown to be an important factor contributing to IR (14), together with its ability to induce a shift toward a more glycolytic phenotype, strongly underlines the positive metabolic effects of this iodothyronine. Taken together, these results lead to its ability to limit or prevent the IR induced by HFD while lowering the serum levels of lipids. Further studies are needed to investigate whether chronic T2 treatment may affect insulin or glucagon secretion to fully address the mechanism by which T2 interferes with glucose homeostasis.

Very recently, the localization and organization of the lipid droplets within the cell have emerged as important qualitative aspects of intramuscular TG storage, together with the identity and properties of the associated proteins that can indeed account for the fate of lipids. ADRP is the predominant lipid droplet-associated protein in skeletal muscle, and a positive relationship between ADRP protein expression and insulin sensitivity has been reported in human skeletal muscle (36). This has led to the hypothesis that up-regulation of ADRP may serve to sequester fatty acids (TGs) within discrete lipid droplets, thus protecting muscle from the detrimental effects of fatty acids on the action of insulin and on glucose tolerance. However, a recent study by Minnaard *et al.* (37) reported a negative correlation between ADRP content and insulin-stimulated glucose uptake in gastrocnemius muscle from ZDF rats as well as in muscle from type 2 diabetic patients. Interestingly, our data extended ADRP localization to the fiber type, and indeed we demonstrated a specific presence of ADRP within fast/glycolytic fibers in the gastrocnemius muscle of HFD rats but predominantly within the slow/oxidative fibers in HFD-T2 rats. Because extrapolating from the relationship between muscle fiber type and ADRP protein expression in whole-muscle homogenates from rats to the situation in humans is an indirect approach, the discrepancies between the above-cited studies may be more apparent than real. Indeed, our results may indicate that the correlation between ADRP and insulin sensitivity relies on the fiber type localization of ADRP and at the same time on the muscle fiber type composition and enrichment. Because extensive data on ADRP fiber type localization and fiber type expression in all the conditions used in the above-mentioned studies have not yet been published (36, 37), the precise role played by ADRP in muscle lipid accumulation in situations of IR remains to be elucidated.

In summary, the work described here provides new insights into the effects of T2 on skeletal muscle metabolism in a situation in which T2 prevents systemic fat accumulation and liver steatosis by stimulating hepatic fatty acid oxidation without harmful effects on either lean muscle or heart mass. In so doing, the present study advances the case for a promotion of muscle glycolytic capacity having metabolic benefits. FJ

This work was partially supported by the following grants: Ministro dell'Istruzione, dell'Università e della Ricerca (MIUR) Cofinanziamento (COFIN) 2008 Protocol 20089SRS2X, MIUR Fondo Investimento Ricerca di Base (FIRB) Medical Research in Italy (MERIT) RBNE08YFN3_003, Regione Campania 2008, and Regione Campania Rete di Spettrometria di Massa.

REFERENCES

1. DeFronzo, R. A., and Tripathy, D. (2009) Skeletal muscle IR is the primary defect in type 2 diabetes. *Diabetes Care* **32,** S157–S163
2. Kelley, D. E., Mokan, M., Simoneau, J. A., and Mandarino, L. S. (1993) Interaction between glucose and free fatty acid metabolism in human skeletal muscle. *J. Clin. Invest.* **92,** 91–98
3. Itani, S. I., Ruderman, N. B., Schmieder, F., and Boden, G. (2002) Lipid-induced IR in human muscle is associated with changes in diacylglycerol, protein kinase C and IκB-α. *Diabetes* **51,** 2005–2011
4. Stump, C. S., Henriksen, E. J., Wei, Y., and Sowers, J. R. (2006) The metabolic syndrome: role of skeletal muscle metabolism. *Ann. Med.* **38,** 389–402
5. Bonen, A., Parolin, M. L., Steinberg, G. R., Calles-Escandon, J., Tandon, N. N., Glatz, J. F., Luiken, J. J., Heigenhauser, G. J., and Dyck, D. J. (2004) Triacylglycerol accumulation in human obesity and type 2 diabetes is associated with increased rates of skeletal muscle fatty acid transport and increased sarcolemmal FAT/CD36. *FASEB J.* **18,** 1144–1146
6. Chabowski, A., Chatham, J. C., Tandon, N. N., Calles-Escandon, J., Glatz, J. F., Luiken, J. J., and Bonen, A. (2006) Fatty acid transport and FAT/CD36 are increased in red but not in white skeletal muscle of ZDF rats. *Am. J. Physiol. Endocrinol. Metab.* **291,** E675–E682
7. Kelley, D. E., Goodpaster, B., Wing, R. R., and Simoneau, J. A. (1999) Skeletal muscle fatty acid metabolism in association with insulin resistance, obesity, and weight loss. *Am. J. Physiol.* **277,** E1130–E1141
8. Kim, J. Y., Hickner, R. C., Cortright, R. L., Dohm, G. L., and Houmard, J. A. (2000) Lipid oxidation is reduced in obese human skeletal muscle. *Am. J. Physiol. Endocrinol. Metab.* **279,** E1039–E1044
9. McGarry, J. D. (2002) Banting lecture 2001: dysregulation of fatty acid metabolism in the etiology of type 2 diabetes. *Diabetes* **51,** 7–18
10. Watt, M. J. (2009) Storing up trouble: does accumulation of intramyocellular triglyceride protect skeletal muscle from insulin resistance? *Clin. Exp. Pharmacol. Physiol.* **36,** 5–11
11. Son, N. H., Yu, S., Tuinei, J., Arai, K., Hamai, H., Homma, S., Shulman, G. I., Abel, E. D., and Goldberg, I. J. (2010) PPARγ-induced cardiolipotoxicity in mice is ameliorated by PPARα deficiency despite increases in fatty acid oxidation. *J. Clin. Invest.* **120,** 3443–3454
12. Hajduch, E., Alessi, D. R., Hemmings, B. A., and Hundal, H. S. (1998) Constitutive activation of protein kinase Bα by membrane targeting promotes glucose and system A amino acid transport, protein synthesis, and inactivation of glycogen synthase kinase 3 in L6 muscle cells. *Diabetes* **47,** 1006–1013
13. Ueki, K., Yamamoto-Honda, R., Kaburagi, Y., Yamauchi, T., Tobe, K., Burgering, B. M., Coffer, P. J., Komuro, I., Akanuma. Y., Yazaki, Y., and Kadowaki, T. (1998) Potential role of protein kinase B in insulin-induced glucose transport, glycogen synthesis, and protein synthesis. *J. Biol. Chem.* **273,** 5315–5322
14. Bodine, S. C., Stitt, T. N., Gonzalez, M., Kline, W. O., Stover, G. L., Bauerlein, R., Zlotchenko, E., Scrimgeour, A., Lawrence, J. C., Glass, D. J., and Yancopoulos, G. D. (2001) Akt/mTOR pathway is a crucial regulator of skeletal muscle hypertrophy and can prevent muscle atrophy in vivo. *Nat. Cell Biol.* **3,** 1014–1019
15. Tremblay, F., and Marette, A. (2001) Amino acid and insulin signaling via the mTOR/p70 S6 kinase pathway. A negative feedback mechanism leading to insulin resistance in skeletal muscle cells. *J. Biol. Chem.* **276,** 38052–38060
16. Belfort, R., Mandarino, L., Kashyap, S., Wirfel, K., Pratipanawatr, T., Berria, R., Defronzo, R. A., and Cusi, K. (2005) Dose-response effect of elevated plasma free fatty acid on insulin signaling. *Diabetes* **54,** 1640–1648
17. Van Loon, L. J., and Goodpaster, B. H. (2006) Increased intramuscular lipid storage in the insulin-resistant and endurance-trained state. *Pflügers Arch.* **451,** 606–616
18. Tanner, C. J., Barakat, H. A., Dohm, G. L., Pories, W. J., MacDonald, K. G., Cunningham, P. R., Swanson, M. S., and Houmard, J. A. (2002) Muscle fiber type is associated with obesity and weight loss. *Am. J. Physiol. Endocrinol. Metab.* **282,** E1191–E1196
19. Levin, M. C., Monetti, M., Watt, M. J., Sajan, M. P., Stevens, R. D., Bain, J. R., Newgard, C. B., Farese, R. V., Sr., and Farese, R. V., Jr. (2007) Increased lipid accumulation and insulin resistance in transgenic mice expressing DGAT2 in glycolytic (type II) muscle. *Am. J. Physiol. Endocrinol. Metab.* **293,** E1772–E1781
20. Izumiya, Y., Hopkins, T., Morris, C., Sato, K., Zeng, L., Viereck, J., Hamilton, J. A., Ouchi, N., LeBrasseur, N. K., and Walsh, K. (2008) Fast/glycolytic muscle fiber growth reduces fat mass and improves metabolic parameters in obese mice. *Cell Metab.* **7,** 159–172
21. Oppenheimer, J. H., Schwartz, H. L., Lane, J. T., and Thompson, M. P. (1991) Functional relationship of thyroid hormone-induced lipogenesis, lipolysis, and thermogenesis in the rat. *J. Clin. Invest.* **87,** 125–132
22. Weinstein, S. P., O'Boyle, E., and Haber, R. S. (1994) Thyroid hormone increases basal and insulin-stimulated glucose transport in skeletal muscle. The role of GLUT4 glucose transporter expression. *Diabetes* **43,** 1185–1189
23. Dimitriadis, G., Parry-Billings, M., Bevan, S., Leighton, B., Krause, U., Piva, T., Tegos, K., Challiss, R. A., Wegener, G., and Newsholme, E. A. (1997) The effects of insulin on transport and metabolism of glucose in skeletal muscle from hyperthyroid and hypothyroid rats. *Eur. J. Clin. Invest.* **27,** 475–483
24. Weinstein, S. P., Watts, J., and Haber, R. S. (1991) Thyroid hormone increases muscle/fat glucose transporter gene expression in rat skeletal muscle. *Endocrinology* **129,** 455–464
25. Dimitriadis, G. D., Leighton, B., Parry-Billings, M., West, D., and Newsholme, E. A. (1989) Effects of hypothyroidism on the sensitivity of glycolysis and glycogen synthesis to insulin in the soleus muscle of the rat. *Biochem. J.* **257,** 369–373
26. Lanni, A., Moreno, M., Lombardi, A., de Lange, P., Silvestri, E., Ragni, M., Farina, P., Baccari, G. C., Fallahi, P., Antonelli, A., and Goglia, F. (2005) 3,5-Diiodo-L-thyronine powerfully reduces adiposity in rats by increasing the burning of fats. *FASEB J.* **19,** 1552–1554
27. De Lange, P., Senese, R., Cioffi, F., Moreno, M., Lombardi, A., Silvestri, E., Goglia, F., and Lanni, A. (2008) Rapid activation by 3,5,3′-L-triiodothyronine of adenosine 5′-monophosphate-activated protein kinase/acetyl-coenzyme a carboxylase and akt/protein kinase B signaling pathways: relation to changes in fuel metabolism and myosin heavy-chain protein content in rat gastrocnemius muscle in vivo. *Endocrinology* **149,** 6462–6470
28. Opie, L. H., and Newsholme, E. A. (1967) The activities of fructose 1,6-diphosphatase, phosphofructokinase and phosphoenolpyruvate carboxykinase in white muscle and red muscle. *Biochem. J.* **103,** 391–399
29. Behan, W. M., Cossar, D. W., Madden, H. A., and McKay, I. C. (2002) Validation of a simple, rapid, and economical technique for distinguishing type 1 and 2 fibres in fixed and frozen skeletal muscle. *J. Clin. Pathol.* **55,** 375–380
30. Koopman, R., Schaart, G., and Hesselink, M. K. (2001) Optimisation of oil red O staining permits combination with immunofluorescence and automated quantification of lipids. *Histochem. Cell Biol.* **116,** 63–68
31. Silvestri, E., Burrone, L., de Lange, P., Lombardi, A., Farina, P., Chambery, A., Parente, A., Lanni, A., Goglia, F., and Moreno, M. (2007) Thyroid-state influence on protein-expression profile of rat skeletal muscle. *J. Proteome Res.* **6,** 3187–3196
32. Talamo, F., D'Ambrosio, C., Arena, S., Del Vecchio, P., Ledda, L., and Zehender, G. (2003) Proteins from bovine tissues and biological fluids: defining a reference electrophoresis map for liver, kidney, muscle, plasma and red blood cells. *Proteomics* **3,** 440–460
33. Scippa, G. S., Rocco, M., Ialicicco, M., Trupiano, D., Viscosi, V., Di Michele, M., Arena, S., Chiatante, D., and Scaloni, A. (2010) The proteome of lentil (*Lens culinaris* Medik.) seeds: discriminating between landraces. *Electrophoresis* **31,** 497-506
34. Qian, W. J., Liu, T., Monroe, M. D. E., Strittmatter, E. F., Jacobs, J. M., Kangas, L. J., Petritis, K., Camp, D. G. 2nd, and Smith, R. D. (2005) Probability-based evaluation of peptide and protein identification from tandem mass spectrometry

and SEQUEST analysis: the human proteome. *J. Proteome Res.* **4,** 53–62
35. Fluck, M., and Hoppeler, H. (2003) Molecular basis of skeletal muscle plasticity—from gene to form and function. *Rev. Physiol. Biochem. Pharmacol.* **146,** 159–216
36. Phillips, S. A., Choe, C. C., Ciaraldi, T. P., Greenberg, A. S., Kong, A. P., Baxi, S. C., Christiansen, L., Mudaliar, S. R., and Henry, R. R. (2005) Adipocyte differentiation-related protein in human skeletal muscle: relationship to insulin sensitivity. *Obes. Res.* **13,** 1321–1329
37. Minnaard, R., Schrauwen, P., Schaart, G., Jorgensen, J. A., Lenaers, E., Mensink, M., and Hesselink, M. K. (2009) Adipocyte differentiation-related protein and OXPAT in rat and human skeletal muscle: involvement in lipid accumulation and type 2 diabetes mellitus. *J. Clin. Endocrinol. Metab.* **94,** 4077–4085
38. Muoio, D. M., and Newgard, C. B. (2006) Obesity-related derangements in metabolic regulation. *Annu. Rev. Biochem.* **75,** 367–401
39. Pimenta, A. S., Gaidhu, M. P., Habib, S., So, M., Fediuc, S., Mirpourian, M., Curi, R., and Ceddia, R. B. (2008) Prolonged exposure to palmitate impairs fatty acid oxidation despite activation of AMP-activated protein kinase in skeletal muscle cells. *J. Cell. Physiol.* **217,** 478–485
40. Randle, P. J., Garland, P. B., Hales, C. N., and Newsholme, E. A. (1963) The glucose fatty-acid cycle. Its role in insulin sensitivity and the metabolic disturbances of diabetes mellitus. *Lancet* **1,** 785–789
41. Saltiel, A. R., and Kahn, C. R. (2001) Insulin signalling and the regulation of glucose and lipid metabolism. *Nature* **414,** 799–806
42. Tremblay, F., Lavigne, C., Jacques, H., and Marette, A. (2001) Defective insulin-induced GLUT4 translocation in skeletal muscle of high fat-fed rats is associated with alterations in both Akt/protein kinase B and atypical protein kinase C (ζ/λ) activities. *Diabetes* **50,** 1901–1910
43. Albright, A., Franz, M., Hornsby, G., Kriska, A., Marrero, D., Ullrich, I., and Varity, L. S. (2000) American College of Sports Medicine position stand. Exercise and type 2 diabetes. *Med. Sci. Sports Exerc.* **32,** 1345–1360
44. Schmitz, K. H., Hannan, P. J., Stovitz, S. D., Bryan, C. J., Warren, M., and Jensen, M. D. (2007) Strength training and adiposity in premenopausal women: strong, healthy, and empowered study. *Am. J. Clin. Nutr.* **86,** 566–572
45. Miyabara, E. H., Aoki, M. S., Soares, A. G., Saltao, R. M., Vilicev, C. M., Passarelli, M., Scanlan, T. S., Gouveia, C. H., and Moriscot, A. S. (2005) Thyroid hormone receptor-β-selective agonist GC-24 spares skeletal muscle type I to II fiber shift. *Cell Tissue Res.* **321,** 233–241

Received for publication February 14, 2011.
Accepted for publication June 2, 2011.